Tellus (1987), *39A*, 95–109

Finite-amplitude stability of a topographically forced wave with Ekman dissipation

By TERRENCE R. NATHAN* and ARTHUR Z. LOESCH, *Department of Atmospheric Science, State University of New York at Albany, Albany, NY 12222, USA*

(Manuscript received August 6, 1985; in final form June 30, 1986)

ABSTRACT

The linear and finite-amplitude stability characteristics of a topographically forced wave are examined in a quasigeostrophic, viscous, barotropic model on a beta-plane. The linear analysis reveals that amplification of a superimposed disturbance is favored when the topographically forced wave is approximately 90° out of phase with the topography. This phase relationship corresponds to flow near topographic resonance. The amplitude evolution of a weakly unstable disturbance is characterized by a monotonic approach to a steady value as it reaches finite amplitude. The nonlinear equilibrating mechanism is the convergence of momentum flux which results from the disturbance interacting with the correction to the topographically forced wave, its higher harmonics, and the form drag induced correction to the mean flow. In the absence of a secondary zonal wavenumber in the disturbance field, the stability threshold for a given set of parameter values is minimized, and equilibration at finite amplitude results solely from the interactions involving the higher harmonics. Finite amplitude instability is shown to exist in certain restricted regions of parameter space.

1. Introduction

Planetary scale stationary waves are an observed feature of the seasonally averaged circulation of the mid-latitude troposphere. As demonstrated by Charney and Eliassen (1949), the existence of such waves can be explained as a natural response of the atmosphere to mechanical forcing by the inhomogeneities in the earth's topography. More recent studies in barotropic and baroclinic models (Egger, 1976; Charney and DeVore, 1979; Roads, 1982; Itoh, 1985) and annulus experiments (Li et al., 1986) have also shown topographic forcing and diabatic heating to be an important component in the generation of stationary waves.

Although baroclinic models provide, in general, better descriptions of the dynamical processes in mid-latitudes, barotropic models are not without relevance, since large-scale stationary waves in winter are, to a large degree, equivalent barotropic in structure (Blackmon et al., 1979; Wallace, 1983). In addition, studies by Grose and Hoskins (1979) and Held (1983) have shown that the linearized barotropic vorticity equation on a sphere yields realistic tropospheric stationary wave patterns.

In an inviscid, barotropic model, Charney and Flierl (1981) have established the linear instability of a topographically forced wave. A connection between the Rayleigh instability of the forced wave and the form drag instability mechanism, encountered by Charney and DeVore (1979) in a study of blocking, was shown to exist at the appropriate limits. However, the absence of nonlinearity in Charney and Flierl's study precludes examination of the dynamics associated with the interaction between the forced stationary wave and *the superimposed disturbance with respect to which it is unstable.* Observational studies (Holopainen, 1978; Lau, 1979) have shown the convergence of momentum flux associated with such interactions to be

* Present affiliation: Department of Earth Sciences, Iowa State University, Ames, Iowa 50011, USA.

important in the stationary wave's long-time average vorticity balance.

Deininger (1981) extended the Charney and Flierl (1981) inviscid study by examining the effects of weak nonlinearity on the temporal evolution of a small, but finite amplitude disturbance superimposed on a stationary, topographically forced basic state wave. Deininger found that the nonlinear feedback between the topographic wave and disturbance produces an *explosive nonlinear instability* for topographic superresonant flow and a vacillation for topographic subresonant flow. In the case of vacillation, the topographic wave remains stationary and 180° out of phase with the topography. Such a phase relationship cannot produce a coupling between the wave fields and mean flow due to topography. Therefore, mountain form drag plays no role in the interaction dynamics between the topographic wave and its superimposed weakly unstable disturbance.

The absence of dissipation represents a fundamental deficiency in the studies of Charney and Flierl (1981) and Deininger (1981). In these studies, the topographically forced wave is either in phase with the topography or 180° out of phase with it. In addition, topographic resonant flow represents a singular point in these studies and was, therefore, excluded from analysis.

In order to provide a more realistic description of the interaction that occurs between a topographically forced wave and its (linearly) unstable disturbance, we extend the study of Deininger (1981) by including the effects of Ekman dissipation. In so doing, the following questions will be addressed: (i) what must the phase of the topographically forced wave be with respect to the topography in order to maximize the energy transfer to the disturbance?; (ii) will the interaction between the topographically forced wave and disturbance be described by a vacillation (as in Deininger) or will the system equilibrate?; (iii) is the explosive nonlinear instability associated with superresonant flow in Deininger's study an artifact of the inviscid dynamics or is it a fundamental result that characterizes the weakly nonlinear interaction between a topographically forced wave and its perturbation?; (iv) what role, if any, will mountain form drag play in the *finite amplitude* evolution of the perturbation field?

As will be shown in answering the above questions, the relative simplicity of the barotropic model, and the systematic use of perturbation methods, will allow for explicit representation of the dynamical balances, and an exact analytical solution to the nonlinear equation governing the temporal evolution of the perturbation field.

2. Governing equations

The nondimensional quasi-geostrophic vorticity equation for a homogeneous, barotropic fluid on an infinite β-plane, in the presence of Ekman dissipation and bottom topography is (see Pedlosky, 1979)

$$\frac{\partial \nabla^2 \Psi}{\partial t} + \beta \frac{\partial \Psi}{\partial x} + J[\Psi, \nabla^2 \Psi + \eta'] = -r\nabla^2 \Psi, \quad (2.1)$$

where

$$\nabla^2 = \partial^2/\partial x^2 + \partial^2/\partial y^2,$$

$$J(a', b') = \frac{\partial a'}{\partial x}\frac{\partial b'}{\partial y} - \frac{\partial a'}{\partial y}\frac{\partial b'}{\partial x}.$$

The scales L, D, V and L/V have been used to nondimensionalize the horizontal lengths, vertical depth, horizontal velocities and time, respectively. In (2.1), x and y are the nondimensional distances in the eastward and northward directions. The geostrophic streamfunction is Ψ while $\eta' = hf_0 L/DV$ represents the topographic variation. The height of the topography is h and f_0 is the Coriolis parameter. The parameter r measures the strength of the Ekman pumping on the upper and lower boundaries and is given by

$$r = \frac{L(2\nu f_0)^{\frac{1}{2}}}{DV}, \quad (2.2a)$$

where ν is the eddy viscosity. The parameter

$$\beta = \frac{\beta' L^2}{V} \quad (2.2b)$$

is the planetary vorticity factor in which β' represents the dimensional, northward gradient of f, i.e., $\beta' = \mathrm{d}f/\mathrm{d}y$.

As in Charney and Flierl (1981), we choose the topography in (2.1) to be of the form

$$\eta'(x) = b\,\mathrm{e}^{ikx} + *, \quad (2.3)$$

where the asterisk denotes the complex conjugate. Without a loss of generality b is assumed real. Topography represented by (2.3) permits an exact solution of (2.1) of the form

$$\Psi_B(x,y) = -Uy + \phi_B(x) \tag{2.4}$$

where

$$\phi_B(x) = |B| b\, e^{i(kx+\chi)} + *, \tag{2.5}$$

$$|B| = \frac{U}{(k^4\delta^2 + r^2k^2)^{\frac{1}{2}}}, \tag{2.6a}$$

$$\chi = \tan^{-1}(r/k\delta), \tag{2.6b}$$

$$\delta = U - \beta/k^2. \tag{2.6c}$$

In view of the fact that $\overline{\phi_{Bx}\eta'} \neq 0$, where the bar denotes a zonal average, the constant zonal flow U must satisfy the form drag equation

$$r(U-d) = \overline{\phi_{Bx}\eta'} \tag{2.7}$$

where d is a zonal momentum source. If d is fixed, multiple equilibria are obtained (e.g., Hart, 1979). If d is allowed to vary, the stability of any basic state can be examined (Buzzi et al., 1984).

A given westerly current, U, flowing over topography (2.3) produces the forced wave ϕ_B given by (2.5) whose amplitude is $b|B|$ and whose phase relative to the mountain is χ. For δ in the range $-\infty < \delta < \infty$, χ lies in the range $\pi > \chi > 0$. The point $\delta = 0$ corresponds to $\chi = \frac{1}{2}\pi$, i.e., the forced wave ridge being 90° west of the topographic ridge. In contrast, in the *absence* of dissipation, superresonant flow ($\delta > 0$) yields an in phase ($\chi = 0$) relationship between the basic wave and mountain, while subresonant flow ($\delta < 0$) yields a 180° out of phase relationship between the basic wave and the mountain ($\chi = \pi$). The inviscid resonant point, $\delta = 0$, where the phase is undefined, represents a singularity and is, therefore, ignored by both Charney and Flierl (1981) and Deininger (1981). As will be shown in Section 3, in the presence of dissipation, the point $\delta = 0$ yields the *strongest* instability of the basic wave (2.5).

In the present study, where an infinite β-plane formulation is used, y-variations in the mountain structure and basic state wave could easily be incorporated without any alteration in the form of the equations governing the zonal momentum and wave fields. It is for this reason that we have chosen to examine the linear and finite-amplitude stability of the algebraically simpler y-independent basic state wave. However, for flow confined to a mid-latitude channel, the presence of dissipation and topography do not permit an exact basic state wave solution. Instead, the basic state itself must be represented as a multi-mode wave spectrum in x and y. In order to obtain an exact basic state solution in the channel configuration, y-variations must be slowly changing, as already shown by Hart (1979).

The stability of (2.4) is examined by taking

$$\Psi(x,y,t) = -Uy + \phi_B(x) + \phi(x,y,t) \tag{2.8}$$

where

$$\phi(x,y,t) = \tilde{\phi}(x,y,t) - u(t)y. \tag{2.9}$$

Substitution of (2.8) into (2.1), together with (2.5), yields the following equation for the wave part of the perturbation field:

$$\begin{aligned}\frac{\partial \nabla^2\tilde{\phi}}{\partial t} &+ \frac{\partial}{\partial x}[U\nabla^2\tilde{\phi} + \beta\tilde{\phi}] + J[\phi_B, \nabla^2\tilde{\phi} + k^2\tilde{\phi}] \\ &- uk^2\frac{\partial\phi_B}{\partial x} + J[\tilde{\phi}, \eta'] + u\frac{\partial\eta'}{\partial x} + r\nabla^2\tilde{\phi} + u\frac{\partial\nabla^2\tilde{\phi}}{\partial x} \\ &+ J[\tilde{\phi}, \nabla^2\tilde{\phi}] = 0.\end{aligned} \tag{2.10}$$

The perturbation form drag equation is

$$\frac{\partial u}{\partial t} + ru = \overline{\tilde{\phi}_x\eta'}^{x,y}. \tag{2.11}$$

3. The linear stability analysis

For infinitesimal disturbances, the nonlinear terms, $J(\tilde{\phi}, \nabla^2\tilde{\phi})$, and $u\nabla^2\tilde{\phi}_x$ in (2.10) can be neglected. The solution for $\tilde{\phi}$ is chosen to be of the form

$$\tilde{\phi}(x,y,t) = e^{i(ly-\sigma t)} \sum_{m=-\infty}^{\infty} P_m e^{i(k_0+mk)x} + *, \tag{3.1}$$

which, provided $l \neq 0$, results in $u = 0$. The special case $l \to 0$ will be discussed later. In (3.1) k_0 is defined as the secondary zonal wavenumber, l is the meridional wavenumber and $\sigma = \sigma_r + i\sigma_i$ is the complex frequency; for amplifying disturbances $\sigma_i > 0$. Substitution of (3.1) into the linearized form of (2.10) results in the following recursion relation

$$P_{m+1} + \alpha_m P_m + \xi_m P_{m-1} = 0, \tag{3.2}$$

where

$$\alpha_m = \frac{-[i\sigma a_m^2 + ik_m(-Ua_m^2 + \beta) - ra_m^2]}{[b - b|B|(-a_{m+1}^2 + k^2)e^{-i\chi}]kl}, \qquad (3.3a)$$

$$\xi_m = \frac{-[b - b|B|(-a_{m-1}^2 + k^2)e^{i\chi}]}{[b - b|B|(-a_{m+1}^2 + k^2)e^{-i\chi}]}, \qquad (3.3b)$$

$$k_m = k_0 + mk, \qquad (3.3c)$$

$$a_m^2 = k_m^2 + l^2. \qquad (3.3d)$$

Based on (3.2), the eigenvalue equation can be written in a continued fraction form (Tung, 1976),

$$-\xi_1/(\alpha_1 - \xi_2/(\alpha_2 - \xi_3/(\cdots)))$$
$$= -(\alpha_0 - \xi_0/(\alpha_{-1} - \xi_{-1}/(\alpha_{-2} - \xi_{-2}/(\cdots)))). \qquad (3.4)$$

Following Tung, the convergence properties of the spectral series (3.1) can be obtained directly from (3.2).

For large m, the two asymptotic solutions of (3.2), which are designated by the superscripts 1 and 2, are:

$$\left|\frac{P_{m+1}^{(1)}}{P_m^{(1)}}\right| \approx \left[\left(\frac{U\sin\chi}{lb^2|B|^2}\right)^2 + \left(\frac{U\cos\chi}{lb|B|}\right)^2\right]^{\frac{1}{2}} m, \qquad (3.5a)$$

$$\left|\frac{P_{m+1}^{(2)}}{P_m^{(2)}}\right| \approx \frac{1}{\left[\left(\frac{U\sin\chi}{lb^2|B|^2}\right)^2 + \left(\frac{U\cos\chi}{lb|B|}\right)^2\right]^{\frac{1}{2}}} \frac{1}{m}, \qquad (3.5b)$$

provided $k_0 \ll mk$. Therefore, as Tung has shown, since the asymptotic solution (3.5b) is rapidly convergent, the series (3.1) will also converge rapidly provided (3.4) is satisfied. The relative rate of convergence will be determined by the size of the bracket in (3.5b). For example, in the vicinity $\delta \sim 0$ (the inviscid resonant point) convergence is enhanced by increasing dissipation and/or increasing the meridional scale of the disturbance field. Weaker zonal flows, or equivalently smaller β/k^2, will also accelerate the convergence. Note also that for $\delta \simeq 0$ the bracket is proportional to b^2 so that, in general, increasing the topographic height will require more terms in the spectral series in order to adequately represent the disturbance field.

For the case $\delta = O(1)$, relatively rapid convergence can still be attained even in the absence of dissipation. As in the case $\delta \approx 0$, long meridional waves enhance convergence. However, in contrast to the case $\delta \approx 0$, the bracket is now proportional to b so that changes in the topographic height will be less effective in influencing the convergence rate.

The last case to be considered is where $k_0 \approx mk$. For this choice of k_0 the asymptotic approximations (3.5) are no longer valid requiring instead an examination of the general solution of the recursion relation (3.2). The procedure is straightforward and the reader is referred to Tung (1976) for details. Briefly, we find that, in general, for $k_0 \approx mk$ the convergence is slow so that such choices of secondary zonal wavenumber are inappropriate for the Lorenz (1972) truncated spectral method to be employed here. The choice $k_0 = 0$ is physically the most relevant because it yields maximum growth rates (by Squires theorem) and produces a zonal flow in (3.1) for $m = 0$.

To investigate the linear stability characteristics of the disturbance field (3.1), the infinite series must be truncated to a suitable number of components so that the essential physical mechanisms can be adequately represented. As defined by Lorenz (1972), the Mth approximation consists of a system of $(2M + 1)$ equations which retain at least two terms when P_m is set equal to zero for $m > M$. Following Lorenz, we choose for analysis the $M = 1$ approximation. The validity of this approximation is checked by comparing the values of b and σ_r corresponding to $\sigma_i = 0$ with those determined from the $M = 2$ approximation.

For the first approximation, (3.2) reduces to,

$$\{i\sigma a_{-1}^2 + ik_{-1}(-Ua_{-1}^2 + \beta) - ra_{-1}^2\}P_{-1}$$
$$- kl\{b - |B|b(-a_0^2 + k^2)e^{-i\chi}\}P_0 = 0, \qquad (3.6a)$$

$$kl\{b - b|B|(-a_{-1}^2 + k^2)e^{i\chi}\}P_{-1}$$
$$+ \{i\sigma a_0^2 + ik_0(-Ua_0^2 + \beta) - ra_0^2\}P_0$$
$$- kl\{b - |B|b(-a_1^2 + k^2)e^{-i\chi}\}P_1 = 0, \qquad (3.6b)$$

$$kl\{b - |B|b(-a_0^2 + k^2)e^{i\chi}\}P_0$$
$$+ \{i\sigma a_1^2 + ik_1(-Ua_1^2 + \beta) - ra_1^2\}P_1 = 0. \qquad (3.6c)$$

A nontrivial solution to (3.6) exists provided,

$$(\sigma - d_1)(\sigma - d_4)(\sigma - d_7)$$
$$= d_2 d_3(\sigma - d_7) + d_5 d_6(\sigma - d_1), \qquad (3.7)$$

where the d_i are complex constants given in Appendix A.

The marginal stability curves, which correspond to $\sigma_i = 0$ in (3.7), have been determined numerically in the (l, b) plane for the following wavenumbers and model parameters characteristic of planetary scale flow: $2 < k < 6$, $0.1 < \beta < 10$, $0 < r < 0.5$, $0.01 < U < 1.5$. The marginal curve characteristics were found to be qualitatively similar for the above range of k and β and, as expected, for a given k, β, r and U, the lowest instability threshold always corresponds to $k_0 = 0$. Therefore, in the following discussion of the marginal curves we choose, as physically representative, $k_0 = 0$, $k = 4$, $\beta = 5$ and vary U and r. For L $\sim$ 5000 km and latitude 45°N, this choice of k and β yields a disturbance zonal wavelength of $\sim$8000 km and a characteristic scaling velocity $V \sim 50$ m/s.

Fig. 1 compares the neutral stability curves for the $M = 1$ and $M = 2$ approximations for $r = 0.1$ and $U = 0.25$. For this choice of U and r, $\chi = 158.2°$ which corresponds to the basic wave ridge 158.2° upstream of the mountain. The first approximation agrees well with the first stability boundary of the second approximation over most of the considered range $2.1 < l < 4.5$, within which the marginal disturbance $(\sigma_i = 0)$ is *stationary*. A minimum in the neutral curve is evident at $l \approx 2.3$. The $M = 1$ approximation fails with respect to the $M = 2$ approximation for l outside this range, where the disturbances may be propagating, or for large topographic heights. These results are consistent with the discussion of the convergence properties presented earlier.

Fig. 2 shows, for the $M = 1$ approximation, that, as expected, an increase in r raises the stability threshold for any l.

We compare next the curves of Fig. 1 with those in Fig. 3 in which $r = 0.1$ but $U = 0.375$. For this choice of r and U, $\chi = 21.8°$ and corresponds to the basic wave ridge 21.8° upstream of the mountain. The instability now occurs over a wider range, $0 < l < 4.45$; the longwave cut-off is absent and the lowest instability threshold now occurs for $l = 0$. The $M = 1$ and $M = 2$ approximations are in agreement in the range $0 < l < 3.7$ within which the disturbances are again stationary along the neutral curve.

The existence of non-zero growth rates when $l \to 0$ in the superresonant example discussed above raises the following question: Is the small l limit, with $k_0 = 0$, a Rayleigh instability associated with the zonally sheared forced wave, or a form drag instability arising from changes in the zonal flow induced by the interaction of $\tilde{\phi}$ with the topography? As demonstrated by Charney

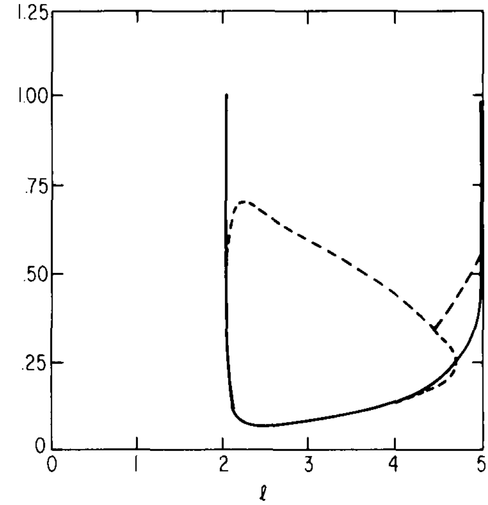

Fig. 1. The neutral stability curves in the (l, b) plane based on the $M = 1$ (solid curves) and $M = 2$ (dashed curves) approximations for $k_0 = 0$, $k = 4$, $\beta = 5$, $U = 0.25$ and $r = 0.1$.

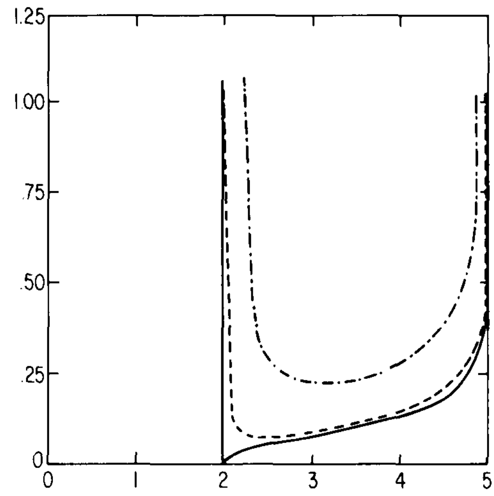

Fig. 2. The neutral stability curves in the (l, b) plane based on the $M = 1$ approximation for $r \to 0$ (solid curves), $r = 0.1$ (dashed curves) and $r = 0.3$ (dashed-dotted curves). k_0, k, β and U are as in Fig. 1.

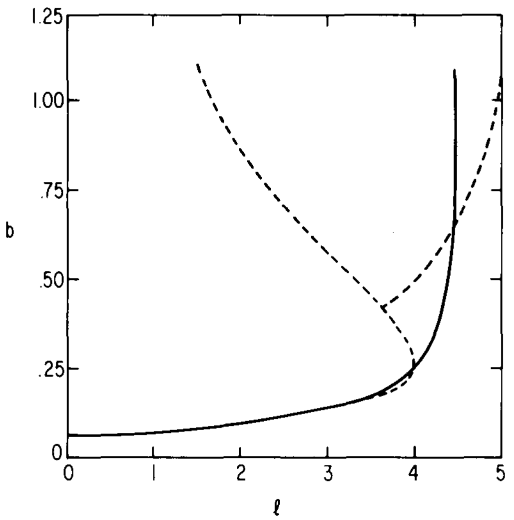

Fig. 3. As in Fig. 1, except $U = 0.3750$.

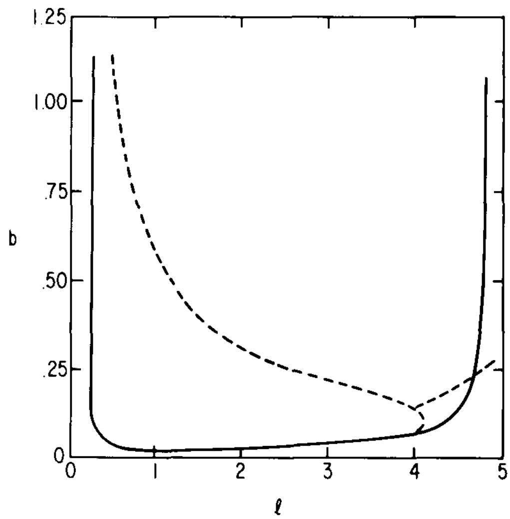

Fig. 4. As in Fig. 1, except $U = 0.3125$.

and Flierl (1981), where an approximation of $\tilde{\phi}$ equivalent to examining the $m = -1$, 0 and 1 modes in (3.1) was used, and more recently by Vallis (1985) using an asymptotic expansion in powers of l, the topography, through the form drag, catalyzes the instability of the mean flow. This is a form drag or orographic instability which, consistent with prior studies (e.g., Charney and DeVore, 1979; Charney and Flierl, 1981; Vallis, 1985), can only occur for superresonant flow (compare Figs. 1, 3 at $l = 0$). Whether the perturbation field is written as $\phi = (P_1 e^{ikx} + P_{-1} e^{-ikx}) + * - uy$, or represented by the $M = 1$ approximation to (3.1), subsequently taking $l \to 0$ in (3.7), *identical* expressions for the critical mountain amplitude, b_c, are obtained.

The examples of the neutral curves given above are for superresonant and subresonant flow regimes well removed from the point $\delta = 0$. We now examine the characteristics of the neutral stability curves for resonant flow, where $\delta = 0$ ($\chi = 90°$). Recall, this parameter setting was excluded from analysis in the studies of Charney and Flierl (1981) and Deininger (1981) due to the singularity arising from the absence of dissipation in their models.

As in Figs. 1 and 3, consider $r = 0.1$, which to satisfy $\delta = 0$, yields $U = 0.3125$. As Fig. 4 illustrates, the instability now has the *lowest* threshold and occurs over the range $0.25 < l < 4.7$. The $M = 1$ and $M = 2$ approximations are in agreement for $0.25 < l < 4.1$ where the disturbance is again stationary along the neutral curve.

In summary, the forced basic wave is most unstable at the resonant point $\delta = 0$ ($\chi = 90°$). The region of instability shifts towards smaller scales as χ increases. On the $M = 1$ marginal curve the disturbances are stationary. The $M = 2$ approximation is in agreement with the lowest stability threshold of the $M = 1$ approximation over most of the unstable range. Disagreement occurs only near the short wave cut-off. For the special case $k_0 = 0$ and $l \to 0$, the Rayleigh or wave instability of the forced basic wave reduces to that of a form drag instability, and can only occur for superresonant ($\delta > 0$) flow. Since highly restricted spatial scales ($k_0 = 0$ and $l \to 0$) and superresonant mean flows ($U > \beta/k^2$) are required for the form drag instability, and since the lowest stability threshold occurs for resonant ($\delta = 0$) flow, the most physically relevant instability mechanism in the present model is the Rayleigh instability associated with the zonally sheared, topographically forced basic wave.

4. The finite-amplitude analysis

The time evolution of the disturbance is examined, for the $M = 1$ approximation, by choosing the topographic height to be near neutral stability, i.e.,

$$b = b_c + \Delta, \quad \Delta \ll 1, \tag{4.1}$$

where b_c is the topographic height required for marginal stability of (3.1). The weak supercriticality, Δ, can be shown to yield a linear growth rate, σ_i, of O($|\Delta|$). Thus, we introduce a long-time scale T defined by

$$T = |\Delta| t \tag{4.2}$$

and transform the time derivative as

$$\frac{\partial}{\partial t} \rightarrow \frac{\partial}{\partial t} + |\Delta| \frac{\partial}{\partial T}. \tag{4.3}$$

Using (4.1) and (4.3) allows (2.10) and (2.11) to be rewritten as

$$\begin{aligned}
&\left[\frac{\partial}{\partial t} + |\Delta| \frac{\partial}{\partial T}\right] \nabla^2 \tilde{\phi} + \frac{\partial}{\partial x}[U \nabla^2 \tilde{\phi} + \beta \tilde{\phi}] \\
&\quad + (b_c + \Delta) \frac{\partial}{\partial x}[|B| e^{i(kx+\chi)} + *] \frac{\partial}{\partial y}[\nabla^2 \tilde{\phi} + k^2 \tilde{\phi}] \\
&\quad - ik(b_c + \Delta)(e^{ikx} - *) \frac{\partial \tilde{\phi}}{\partial y} \\
&\quad - uk^2(b_c + \Delta) \frac{\partial}{\partial x}[|B| e^{i(kx+\chi)} + *] \\
&\quad + u(b_c + \Delta) \frac{\partial}{\partial x}(e^{ikx} + *) + r \nabla^2 \tilde{\phi} + J[\tilde{\phi}, \nabla^2 \tilde{\phi}] \\
&\quad + u \frac{\partial}{\partial x} \nabla^2 \tilde{\phi} = 0,
\end{aligned} \tag{4.4}$$

$$\left[\frac{\partial}{\partial t} + |\Delta| \frac{\partial}{\partial T}\right] u + ru = (b_c + \Delta) \overline{\tilde{\phi}_x (e^{ikx} + *)}^{x, y}. \tag{4.5}$$

To balance the weak instability with nonlinearity in (4.4) we choose asymptotic expansion for $\tilde{\phi}$ and u of the form,

$$\begin{aligned}
&\tilde{\phi}(x, y, t, T, |\Delta|) \\
&\quad = |\Delta|^{\frac{1}{2}} \tilde{\phi}^{(1)}(x, y, t, T) + |\Delta| \tilde{\phi}^{(2)}(x, y, t, T) + \cdots
\end{aligned} \tag{4.6a}$$

$$u(t, T, |\Delta|) = |\Delta|^{\frac{1}{2}} u^{(1)}(t, T) + |\Delta| u^{(2)}(t, T) + \cdots. \tag{4.6b}$$

Substituting (4.6a) and (4.6b) into (4.4) and (4.5) results in a sequence of linear problems in increasing powers of $|\Delta|$.

To lowest order we have

$$\begin{aligned}
&\frac{\partial \nabla^2 \tilde{\phi}^{(1)}}{\partial t} + \frac{\partial}{\partial x}[U \nabla^2 \tilde{\phi}^{(1)} + \beta \tilde{\phi}^{(1)}] \\
&\quad + b_c \frac{\partial}{\partial x}[|B| e^{i(kx+\chi)} + *] \frac{\partial}{\partial y}(\nabla^2 \tilde{\phi}^{(1)} + k^2 \tilde{\phi}^{(1)}) \\
&\quad - ikb_c(e^{ikx} - *) \frac{\partial \tilde{\phi}^{(1)}}{\partial y} \\
&\quad - u^{(1)} k^2 b_c \frac{\partial}{\partial x}[|B| e^{i(kx+\chi)} + *] \\
&\quad + u^{(1)} b_c \frac{\partial}{\partial x}(e^{ikx} + *) + r \nabla^2 \tilde{\phi}^{(1)} = 0,
\end{aligned} \tag{4.7}$$

$$\frac{\partial u^{(1)}}{\partial t} + ru^{(1)} = b_c \overline{\tilde{\phi}_x^{(1)} (e^{ikx} + *)}^{x, y}, \tag{4.8}$$

which specifies the disturbance field on the marginal curve, b_c. With $k_0 \neq 0$ and/or $l \neq 0$, the three mode truncation yields $u^{(1)} = 0$ since $\overline{\tilde{\phi}_x^{(1)} \eta'}^{x, y} = 0$, thus allowing the amplitudes P_{-1} and P_1 to be rewritten in terms of P_0 using (3.6). Therefore, the neutral solution can be written in the form,

$$\tilde{\phi}^{(1)} = \sum_{n=-1}^{1} |L_n| P_0(T) e^{i(\hat{\theta}_n + \gamma_n)} + *, \tag{4.9}$$

where

$$\hat{\theta} = (k_0 + nk)x + ly - \sigma_r t, \tag{4.10}$$

and $|L_n|$ and γ_n are given in Appendix B. Although, as shown in Section 3, maximum growth rates correspond to the secondary zonal wavenumber $k_0 = 0$, we retain k_0 in (4.9) in order to compare the nonlinear equilibrating mechanisms that result when $k_0 \neq 0$ with those for $k_0 = 0$.

We now focus on the O($|\Delta|$) problem where the nonlinearity arising from the self-interaction of the perturbation field (4.9) first becomes evident. Collecting the O($|\Delta|$) terms in (4.4) and (4.5), and evaluating them in terms of previously determined fields yields,

$$\begin{aligned}
&\frac{\partial \nabla^2 \tilde{\phi}^{(2)}}{\partial t} + \frac{\partial}{\partial x}[U \nabla^2 \tilde{\phi}^{(2)} + \beta \tilde{\phi}^{(2)}] \\
&\quad + b_c \frac{\partial}{\partial x}[|B| e^{i(kx+\chi)} + *] \frac{\partial}{\partial y}[\nabla^2 \tilde{\phi}^{(2)} + k^2 \tilde{\phi}^{(2)}] \\
&\quad - ikb_c(e^{ikx} - *) \frac{\partial \tilde{\phi}^{(2)}}{\partial y} \\
&\quad - u^{(2)} k^2 b_c \frac{\partial}{\partial x}[|B| e^{i(kx+\chi)} + *] \\
&\quad + u^{(2)} b_c \frac{\partial}{\partial x}(e^{ikx} + *) + r \nabla^2 \tilde{\phi}^{(2)}
\end{aligned}$$

$$= lP_0^2\{|L_{-1}|(a_{-1}^2 - a_0^2)(k_{-1} - k_0)\,e^{i\gamma_{-1}}e^{i\theta_{-1}}$$
$$+ |L_1|(a_1^2 - a_0^2)(k_1 - k_0)\,e^{i\gamma_1}e^{i\theta_1}\} + *$$
$$- l|P_0|^2\{|L_{-1}|(a_{-1}^2 - a_0^2)(k_{-1} - k_0)\,e^{-i\gamma_{-1}}$$
$$+ |L_1|(a_1^2 - a_0^2)(k_1 - k_0)\,e^{i\gamma_1}\}\,e^{ikx} + *$$
$$+ iku^{(2)}[|B|\,e^{i\chi}k^2 - 1]\,b_c\,e^{ikx} + *, \tag{4.11}$$

$$ru^{(2)} = b_c\,\overline{\tilde{\phi}_x^{(2)}(e^{ikx} + *)}. \tag{4.12}$$

Only those terms consistent with the original truncation have been retained. The three forcing terms on the right-hand side of (4.11) are nonresonant and produce the particular solutions,

$$\tilde{\phi}_B^{(2)}(x, T) = |F_B||P_0(T)|^2\,e^{i(kx + \chi + \zeta)} + *, \tag{4.13}$$

$$\tilde{\phi}_M^{(2)}(x, T) = u^{(2)}(T)|M_B|\,e^{i(kx + \chi + \zeta_B)} + *, \tag{4.14}$$

$$\tilde{\phi}_f^{(2)}(x, y, t, T) = \sum_{m=-1}^{1} f_m^{(2)}\,P_0^2(T)\,e^{i\bar{\theta}_m} + *, \tag{4.15}$$

where

$$\bar{\theta}_m = mkx + 2(k_0 x + ly - \sigma_r t). \tag{4.16}$$

The real constants $|F_B|$, ζ, $|M_B|$ and ζ_B, and the complex constants $f_m^{(2)}$, are given in Appendix C.

The particular solution (4.13), which arises from the self-interaction of the disturbance field (4.9), represents an $O(|\Delta|)$ correction to the topographically forced wave and is, at any instant, proportional to the modulus of the disturbance amplitude squared, $|P_0|^2$. This result differs from the inviscid analysis of Deininger (1981) where the correction to the basic state wave is proportional to the departure of the amplitude, P_0, from its initial value. This difference between the inviscid and viscous cases has also been found in the context of the baroclinic stability problem (Pedlosky, 1970).

The particular solution (4.14) represents another $O(|\Delta|)$ basic wave correction which, in contrast to (4.13), results from the interaction of the $O(|\Delta|)$ zonal flow with both the basic wave and topography. Upon collecting the $O(|\Delta|)$ terms in the zonal flow equation (4.5), it can be shown that the form drag term arising from the interaction of the basic wave correction (4.13), with the topography, is responsible for the zonal flow correction $u^{(2)}$ which is *diagnostically* related to $|P_0|^2$, viz.,

$$u^{(2)}(T) = Q|P_0(T)|^2 \tag{4.17}$$

where,

$$Q = \frac{-k2b_c|F_B|\sin(\chi + \zeta)}{r + 2b_c k|M_B|\sin(\chi + \zeta_B)}. \tag{4.18}$$

This result differs markedly from Deininger's (1981) inviscid analysis where, due to the absence of dissipation, the basic state wave correction remains in phase with the topography so that form drag induced zonal flow changes are not possible. Therefore, the only nonlinear mechanism by which the basic state wave can be corrected in Deininger's study is through the self-advection of the disturbance field.

The remaining particular solution, (4.15), contains in its spatial structure higher harmonics in k_0 and l produced at $O(|\Delta|)$ through the self-interaction of the disturbance field, (4.9). This solution is proportional to the disturbance amplitude squared, and will be shown later to play a vital role in the nonlinear equilibration of the disturbance.

Before proceeding to the $O(|\Delta|^{3/2})$ problem where the evolution equation for P_0 is determined, the total streamfunction field is reconstructed to $O(|\Delta|)$ using (4.1), (4.6a), (4.9), and (4.13)–(4.15):

$$\Psi(x, y, t, T, |\Delta|)$$
$$= -Uy + \{(b_c + \Delta)|B| + |\Delta|(|F_B||P_0|^2\,e^{i\zeta}$$
$$+ u^{(2)}|M_B|\,e^{i\zeta_B})\,e^{i(kx + \chi)} + *\}$$
$$+ |\Delta|^{\frac{1}{2}}\left[\sum_{m=-1}^{1} |L_m|P_0\,e^{i(\theta_m + \gamma_m)} + *\right]$$
$$+ |\Delta|\left[\sum_{m=-1}^{1} f_m^{(2)}P_0^2\,e^{i\bar{\theta}_m} + *\right]. \tag{4.19}$$

Since $|B| > 0$, it can be shown that the basic wave correction (4.13) which arises from the self-interaction of the disturbance (4.9), is stabilizing provided $|F_B| \neq 0$ and $[\cos\zeta - \tan(kx + \chi)\sin\zeta] < 0$, i.e., when the amplifying disturbance acts to reduce the basic wave amplitude. When $[\cos\varphi - \tan(kx + \chi)\sin\varphi] > 0$ the basic wave correction, (4.13), produces a further destabilization of the basic wave. The interaction of the corrected zonal flow, $u^{(2)}$, with both the basic wave and topography results in stabilization of the basic flow when $u^{(2)}[\cos\zeta_B - \tan(kx + \chi) - \sin\zeta_B] < 0$. The case $|F_B| = 0$ occurs when $k_0 = 0$ which, recall, is the most physically relevant choice for k_0 since growth rates are maximized. Therefore, when $k_0 = 0$ the basic wave corrections, (4.13) and (4.14), vanish so that equilibration of the perturbation can only come about via nonlinear interactions involving the higher harmonics, given by (4.15). This will become evident at $O(|\Delta|^{3/2})$.

The basic state structure of the streamfunction field, (4.19), differs in several respects from that obtained by Deininger (1981). First, in Deininger's inviscid analysis, the basic wave correction is *always* in phase with the topography; the basic wave is in phase with the topography for superresonant flow or 180° out of phase for subresonant flow. Thus, mountain form drag plays no role in the interaction between the basic wave state and disturbance. Furthermore, it is for superresonant flow where Deininger finds that the basic wave correction leads to an explosive nonlinear instability. In this study, due to the presence of Ekman dissipation, the phase of both the basic wave and its correction are always out of phase with each other and with the topography. Therefore, provided $k_0 \neq 0$, nonlinear stabilization due to the basic state wave corrections, which is manifested through $|F_B|$, $|M_B|$, ζ and ζ_B, is no longer a simple matter of the mean flow being subresonant or superresonant, but instead, is now determined by a complicated relationship among *all* the model parameters. A further discussion of the finite amplitude stability characteristics is presented at the next order where the evolution equation for the disturbance amplitude is determined.

Collecting the $O(|\Delta|^{3/2})$ terms in (4.4) and (4.5), evaluating them in terms of previously determined fields, and then removing the secular terms using standard techniques (see, for example, Deininger (1981)), we find that $u^{(3)} = 0$ and obtain the evolution equation for the perturbation amplitude:

$$\frac{\mathrm{d}P_0}{\mathrm{d}T} + (\eta_r + i\eta_i)P_0 + (N_r + iN_i)P_0|P_0|^2 = 0. \quad (4.20)$$

The constants η and N are given in Appendix D. From (4.20) the equilibration equation for $|P_0|$ can be derived, i.e.,

$$\frac{\mathrm{d}|P_0|^2}{\mathrm{d}T} = -2|P_0|^2\left[\frac{\Delta}{|\Delta|}\eta_r + N_r|P_0|^2\right]. \quad (4.21)$$

This equation is identical in form to that obtained by Landau (1944). Equations having the form of (4.20) have also been found in quasi-geostrophic models dealing with the finite-amplitude stability of baroclinic zonal flow without beta (Pedlosky, 1970 and Drazin, 1972) and with beta (Romea, 1977). More recently, Burns and Maslowe (1983) have shown that in the presence of dissipation, the weakly nonlinear evolution of a disturbance superimposed on an unstable zonal shear flow is also governed by an equation having the form of (4.20).

In (4.21), $\eta_r < 0$ corresponds to linear growth. The finite amplitude behavior of the disturbance is determined by N_r, which is comprised of a contribution from the feedback with the basic wave correction (N_B), a part arising from the interaction of the disturbance with the form drag induced $O(|\Delta|)$ correction to the mean flow (N_D), and a term due to interactions involving the higher harmonics (N_H), i.e.,

$$N_r = N_B + N_H + N_D. \quad (4.22)$$

When $k_0 = 0$, both N_B and N_D vanish so that $N_r = N_H$. Finite-amplitude stability requires $N_r > 0$. Although the three mode truncation yields excellent estimates of b_c, σ_r and σ_i for a variety of parameter settings, the corresponding estimates of the nonlinear coupling coefficient, N, may not be as good. In principle the estimate of N based on three modes should be compared against values determined from less severe truncations; this would be an extremely arduous task. Therefore, the calculations of N that follow are based on three modes, realizing that an estimate of N based on such an approximation may be not representative for all parameter settings. However, *regardless of the number of modes retained in the disturbance field (4.9), the form of the evolution equation (4.20) remains the same.*

Clearly, from (4.21), a nonlinear equilibration of the disturbance is possible only when $N_r > 0$. Negative values of N_r may result from (i) the inadequacy of the three-mode truncation in estimating N_r, or (ii) parameter settings where the weakly nonlinear theory is no longer valid, i.e., where the time scale of the nonlinearity is shorter than that of the linear instability requiring, instead, a full spectral-numerical treatment of the dynamics.

The solution to (4.21) is

$$|P_0(T)|^2 = \frac{|P_0(0)|^2\,\mathrm{e}^{-2\eta_r T}}{1 - (N_r/\eta_r)|P_0(0)|^2(\mathrm{e}^{-2\eta_r T} - 1)} \quad (4.23)$$

and describes, for $\eta_r < 0$ and $N_r > 0$, a monotonic approach of the disturbance amplitude modulus to the steady value

$$|P_0(\infty)|^2 = -\eta_r/N_r. \tag{4.24}$$

An equation for the evolution of the phase can also be derived from (4.20). Writing P_0 as

$$P_0(T) = W(T)\,e^{i\theta(T)}, \tag{4.25}$$

it can be shown (see, for example, Romea (1977)) that

$$\theta(T) = -\eta_i T - N_i \int_0^T W^2(T)\,dT. \tag{4.26}$$

The first term on the right-hand side of (4.26) is the linear phase correction arising from the O($|\Delta|$) departure of the basic wave amplitude from its marginal value. The second term represents the nonlinear phase correction, which approaches a constant value as the wave equilibrates. Depending on the choice of wavenumbers and model parameter values, N_i can act to either slow down or speed up the linear propagation of the disturbance as it evolves in time. The phase correction, θ, adds an eastward (westward) component to the total phase when $\eta_i > 0$ (< 0) and $N_i > 0$ (< 0).

Fig. 5 depicts, for $r = 0.1$ ($\chi = 158.2°$) and $r = 0.3$ ($\chi = 128.81°$), the variation of $|P_0(\infty)|^2$ with l for the same values of U, β, k_0 and k as in Fig. 1. Recall, $k_0 = 0$ yields $N_B = N_D = 0$ so that equilibration of the disturbance amplitude results solely from the nonlinear interactions involving the higher harmonics (provided $N_r = N_H > 0$). The above parameter setting corresponds to *subresonant* flow away from the vicinity of the resonant point $\delta = 0$. Comparing values of $|P_0(\infty)|^2$ corresponding to the integer values $l = 3$ and $l = 4$ reveals that neither wavenumber is significantly dominant at finite amplitude when $r = 0.1$. However, when $r = 0.3$, the smaller meridional scale corresponding to $l = 4$ yields slightly larger equilibrated values of $|P_0(\infty)|^2$ than that for $l = 3$. Generally, there is an overall increase in $|P_0(\infty)|^2$ with larger r.

The increase in $|P_0(\infty)|$ with larger r shown in Fig. 5 can be qualitatively understood using physical arguments recently discussed by Reinhold (1986). Generally, a disturbance is less efficient in extracting energy from the basic state with increased dissipation, as manifested by a reduction in both the growth rate and horizontal phase tilt of the disturbance. Thus, in order to achieve the momentum transport necessary to balance energy extraction from the basic state and energy dissipation due to friction, a larger disturbance amplitude may be required. Although there are exceptions which must be determined by detailed calculations, larger equilibrated amplitudes in regions of parameter space where growth rates are reduced should not be surprising.

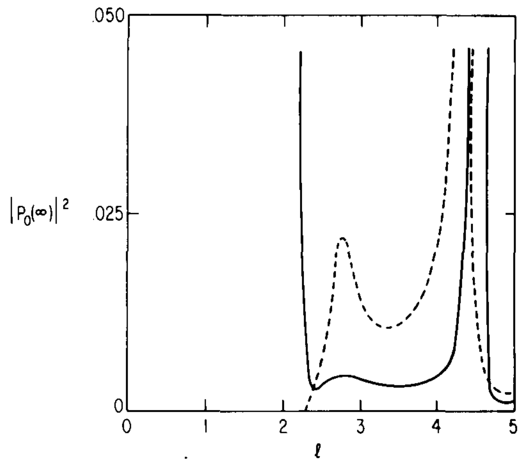

Fig. 5. $|P_0(\infty)|^2$ versus l based on the $M = 1$ approximation for $r = 0.1$ (solid curves) and $r = 0.3$ (dashed curves). Parameters are: $k_0 = 0$, $k = 4$, $\beta = 5$ and $U = 0.25$.

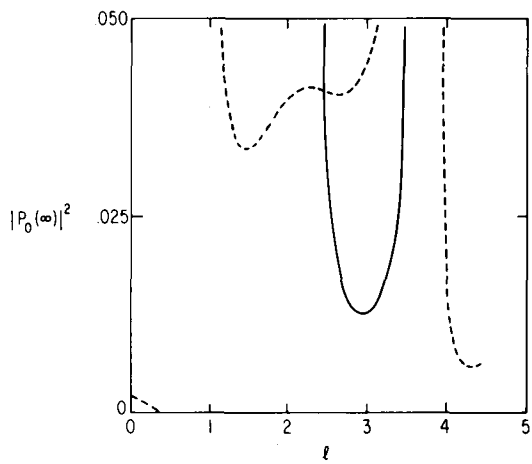

Fig. 6. As in Fig. 5, except $U = 0.3750$.

In Fig. 6, the variations of $|P_0(\infty)|^2$ as a function of l are shown for *superresonant* flow removed from resonance. The parameters U, β,

k_0 and k are the same as in Fig. 5. $|P_0(\infty)|^2$ results only from interactions between the disturbance and its higher harmonics, as in Fig. 5. However, comparing Fig. 6 with Fig. 5 reveals two important differences: first, for $r = 0.1$ ($\chi = 21.8°$) finite-amplitude stability and, therefore, existence of $|P_0(\infty)|^2$ is evident over only $\sim 50\%$ of the linearly unstable l range, corresponding to the smaller meridional scales. Second, increasing the dissipation strength to $r = 0.3$ ($= 50.19°$) increases $|P_0(\infty)|^2$ and expands its range towards smaller l. The limit $l \to 0$ is characterized by finite-amplitude instability when $r = 0.1$ and the *smallest* value of $|P_0(\infty)|^2$ when $r = 0.3$. Therefore, the largest equilibrated values of the disturbance amplitude occur for those meridional wavenumbers where the linear instability of the forced basic wave is of the Rayleigh type.

Finally, the behavior of $|P_0(\infty)|^2$ as a function of l is depicted for resonant flow ($\delta = 0$) in Fig. 7. Note that irrespective of the dissipation strength, $\chi = 90°$ when $\delta = 0$. The values of U, β, k_0 and k used in calculating $|P_0(\infty)|^2$ are the same as in Fig. 4. Since $k_0 = 0$, the nonlinear equilibration of $|P_0|^2$ is again due to the higher harmonics. As shown in Fig. 7, for $r = 0.1$, $|P_0(\infty)|^2$ exists over a relatively broad range of l corresponding to the larger meridional wavenumbers. In addition, as in Figs. 5 and 6, there is a general increase in $|P_0(\infty)|^2$ for larger r.

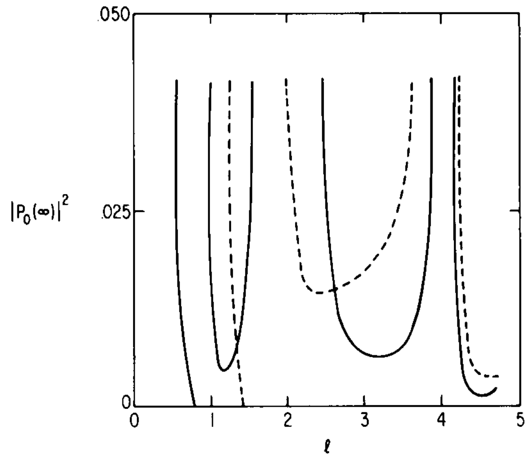

Fig. 7. As in Fig. 5, except $U = 0.3125$.

5. Summary and conclusions

The preceding analysis examines the finite amplitude stability of a topographically forced wave in the presence of Ekman dissipation. A superimposed disturbance, represented as a spectral series, is truncated first to three modes and then to five modes and the neutral stability curves compared. For a weakly unstable basic wave flow, the finite amplitude time evolution equation is also derived for the three mode disturbance.

Flows both away from and at the (topographic) resonant point $\delta = 0$ have been considered. In all cases the marginal stability curves of the three mode approximation are in close agreement with the lowest stability curves of the five mode approximation over most of the unstable wavenumber range. Increasing dissipation raises the stability threshold for *all* meridional wavenumbers. As the resonant point is approached, linear instability can occur for smaller topographic heights and over a wider range of meridional wavenumbers. Resonant basic flow is, therefore, the most favored for disturbance amplification. Irrespective of the dissipation strength, resonant flow corresponds to the linearly determined phase of the topographically forced wave ridge being 90° upstream from the topographic ridge.

In the special case where the disturbance contains a zonal flow component which depends only on time (i.e., $l \to 0$), and the flow is superresonant (i.e., $\delta > 0$), the instability that results is due to the form drag. In contrast, when the disturbance is characterized by a meridional wavenumber $l \neq 0$, the more general Rayleigh or wave instability of the forced basic wave can occur for subresonant ($\delta < 0$), superresonant ($\delta > 0$), or resonant flow ($\delta = 0$). In each case the instability is maximized in the absence of the secondary zonal wavenumber, k_0, in the disturbance field. For a given l and k_0, the lowest stability threshold always occurs for the resonant flow, a parameter setting which precludes the possibility of form drag instability. It is for these reasons that the Rayleigh instability of the forced basic wave is the most relevant to the amplification and finite amplitude evolution of the mid-latitude disturbances examined in this study.

The finite amplitude analysis yields a *first* order in time equation for the complex amplitude of the disturbance field. Provided the real part of the nonlinear couling coefficient, N, is greater than zero, the amplitude modulus of the disturbance field is governed by a Landau (1944) S-curve equilibration. If the imaginary part of N is positive (negative), the nonlinear phase correction is such as to decelerate (accelerate) the disturbance field as it evolves in time.

The explosive nonlinear instability which occurs whenever $\delta > 0$ in Deininger's (1981) inviscid, weakly nonlinear analysis is not reproduced here. Instead, such an instability, characterized by the real part of N less than zero, occurs in this study only in certain restricted regions of parameter space. In addition, due to the self-interaction of the disturbance field, there is a *time-independent* correction to the phase of the forced basic wave, which is not produced in Deininger's study. The differences are apparently due to dissipation which produces a phase shift in the forced basic wave state relative to the topography.

The nonlinear equilibrating mechanism in this study is the convergence of momentum flux which results from the disturbance field interacting with its higher harmonics, the $O(|\Delta|)$ correction to the basic state wave, and the form drag induced $O(|\Delta|)$ correction to the mean flow. However, in the absence of k_0 in the disturbance field, equilibration at finite amplitude results *only* from the interactions involving the higher harmonics.

The barotropic instability of a stationary, topographically forced basic state wave, in the presence of Ekman dissipation, has been shown to occur for any zonal flow U, provided the basic wave amplitude is sufficiently large. Based upon the broad range of U over which the zonally varying basic state may be unstable, and since observational studies of the Northern Hemisphere (e.g., Blackmon et al., 1979; Wallace, 1983) have shown that the large scale stationary waves in winter are, to a large extent, equivalent barotropic in structure, it is possible that the barotropic instability examined here may play an important rôle in limiting the amplitude of the stationary waves in the troposphere to the observed range of values. In addition, it has been shown that for a stationary, topographically forced basic state wave, whose amplitude is supercritical with respect to the lowest stability threshold by a small but finite amount Δ, the superimposed disturbance field, to which the zonally varying basic flow is weakly unstable, is characterized by a low $[O(|\Delta|)]$ frequency. Such low frequency variability of the normal modes arising from the barotropic instability of a stationary zonally varying flow has also been found by Simmons et al. (1983) in a global barotropic model. Thus, as suggested by Simmons et al., much of the low frequency variability of the geopotential height field during the winter season may arise from the barotropic instability of zonally varying time-mean states.

The foregoing analysis also describes one of the basic nonlinear mechanisms by which forced stationary waves and travelling disturbances interact in the atmosphere, i.e., through the convergence of momentum flux. This mechanism has been shown by Lau (1979) and Youngblut and Sasamori (1980) to play an important part in the long-time average vorticity balance of the stationary waves in the troposphere. Consistent with these studies, the convergence of momentum flux arising from the self-advection of the (travelling) disturbance field has been shown to have a dissipative effect on the stationary basic wave, provided the nonlinear coupling coefficient arising from the feedback with the basic wave correction is positive ($N_B > 0$). The basic wave correction *decreases* the imposed basic wave amplitude at a rate proportional to the disturbance amplitude modulus squared. As $T \to \infty$, the disturbance amplitude modulus monotonically approaches a steady value, with the forced stationary wave in a more stable state than originally imposed.

Although this study focuses on the linear and finite amplitude stability characteristics of forced zonally varying flow in a barotropic atmosphere, it should also be noted that the instability of such flow is equally important to the fluctuation activity in the oceans, as already discussed by Vallis (1985). However, whether the focus is on the dynamics of the atmosphere or ocean, several additional model features must be incorporated in future studies. One of the more important is to examine the linear and nonlinear stability characteristics of a baroclinic wave state which is forced by *multi-mode* topography. The dynamics of disturbances superimposed on stationary, zonally localized background flow in the presence of a vertically sheared zonal flow can then be examined. Moreover, disturbances could draw on both the potential and kinetic energy of the basic state. Such a problem is currently being studied.

6. Acknowledgements

The authors thank the reviewers for their helpful comments and suggestions, and, in particular, we thank one reviewer for bringing to our attention an inconsistency in the original manuscript. Thanks are also due Ms. Linda Claussen for the typing of the manuscript. This work was supported by the National Science Foundation under Grants ATM-8117403 and ATM-8411327. Acknowledgement is also made to the National Center for Atmospheric Research, which is sponsored by the National Science Foundation, for the computer time used in this research.

7. Appendix A

Explicit representation of the complex coefficients d_i in eq. (3.7)

$$d_1 = \frac{-k_{-1}}{a_{-1}^2}(-Ua_{-1}^2 + \beta) - ir, \tag{A1}$$

$$d_2 = \frac{iklb}{a_{-1}^2}[1 - |B|(-a_0^2 + k^2)e^{-i\chi}], \tag{A2}$$

$$d_3 = \frac{-iklb}{a_0^2}[1 - |B|(-a_{-1}^2 + k^2)e^{i\chi}], \tag{A3}$$

$$d_4 = \frac{-k_0}{a_0^2}(-Ua_0^2 + \beta) - ir, \tag{A4}$$

$$d_5 = \frac{iklb}{a_0^2}[1 - |B|(-a_1^2 + k^2)e^{-i\chi}], \tag{A5}$$

$$d_6 = \frac{-iklb}{a_1^2}[1 - |B|(-a_0^2 + k^2)e^{i\chi}], \tag{A6}$$

$$d_7 = \frac{-k_1}{a_1^2}(-Ua_1^2 + \beta) - ir, \tag{A7}$$

$$a_n^2 = k_n^2 + l^2. \tag{A8}$$

8. Appendix B

Expressions for $|L_n|$ and γ_n in eq. (4.9)

The $|L_n|$ and γ_n ($n = 1, -1$) are,

$$|L_n| = [(L_n^{(R)})^2 + (L_n^{(I)})^2]^{\frac{1}{2}}/e_5^{(n)}, \tag{B1}$$

$$\gamma_n = \tan^{-1}\left[\frac{L_n^{(I)}}{L_n^{(R)}}\right], \tag{B2}$$

where,

$$|L_n^{(R)}| = \frac{-nklb_c}{a_n^2}(e_1^{(n)}e_3^{(n)} - e_2^{(n)}e_4^{(n)}), \tag{B3}$$

$$|L_n^{(I)}| = \frac{nklb_c}{a_n^2}(e_1^{(n)}e_4^{(n)} + e_2^{(n)}e_3^{(n)}), \tag{B4}$$

$$e_1^{(n)} = -|B|(-a_0^2 + k^2)\sin(n\chi), \tag{B5}$$

$$e_2^{(n)} = 1 - |B|(-a_0^2 + k^2)\cos(n\chi), \tag{B6}$$

$$e_3^{(n)} = \sigma_r + \frac{k_n(-Ua_n^2 + \beta)}{a_n^2}, \tag{B7}$$

$$e_4^{(n)} = r, \tag{B8}$$

$$e_5^{(n)} = (e_3^{(n)})^2 + r^2, \tag{B9}$$

$$|L_0| = 1, \tag{B10}$$

$$\gamma_0 = 0. \tag{B11}$$

9. Appendix C

Explicit representation of $|F_B|$, ζ, $|M_B|$, $|\zeta_B$ and $f_m^{(2)}$

$|F_B|$ and ζ are,

$$|F_B| = [(F_B^{(R)})^2 + (F_B^{(I)})^2]^{\frac{1}{2}}, \tag{C1}$$

$$\zeta = \tan^{-1}\left[\frac{F_B^{(I)}}{F_B^{(R)}}\right], \tag{C2}$$

where

$$F_B^{(R)} = \frac{|B|l}{Uk}\{|L_1|(a_1^2 - a_0^2)(k_1 - k_0)\sin\gamma_1 - |L_{-1}|(a_{-1}^2 - a_0^2)(k_{-1} - k_0)\sin\gamma_{-1}\}, \tag{C3}$$

$$F_B^{(I)} = \frac{-|B|l}{Uk}\{|L_1|(a_1^2 - a_0^2)(k_1 - k_0)\cos\gamma_1 + |L_{-1}|(a_{-1}^2 - a_0^2)(k_{-1} - k_0)\cos\gamma_{-1}\}. \tag{C4}$$

$|M_B|$ and ζ_B are,

$$|M_B| = \frac{b_c|B|}{U}[1 + |B|^2k^4 - 2|B|k^2\cos\chi]^{\frac{1}{2}}, \tag{C5}$$

$$\zeta_B = \tan^{-1}\left[\frac{-|B|k^2\sin\chi}{(1 - |B|k^2\cos\chi)}\right]. \tag{C6}$$

The $f_m^{(2)}$ are,

$$f_1^{(2)} = -[A_6 A_3 A_8 - (A_2 A_3 - A_4 A_1) A_9]/[A_6 A_1 A_5 + (A_2 A_3 - A_4 A_1)], \quad \text{(C7)}$$

$$f_0^{(2)} = [A_9 - A_7 f_1^{(2)}]/A_6, \quad \text{(C8)}$$

$$f_{-1}^{(2)} = [A_8 - A_2 f_0^{(2)}]/A_1, \quad \text{(C9)}$$

where,

$$A_1 = -r\bar{a}_{-1}^2 + i[\bar{a}_{-1}^2 2\sigma_r + k_{-1}(U\bar{a}_{-1}^2 + \beta)], \quad \text{(C10)}$$

$$A_2 = 2kl|B|b_c(-\bar{a}_0^2 + k^2)\mathrm{e}^{-i\chi} - 2b_c kl, \quad \text{(C11)}$$

$$A_3 = -2kl|B|b_c(-\bar{a}_{-1}^2 + k^2)\mathrm{e}^{i\chi} + 2b_c kl, \quad \text{(C12)}$$

$$A_4 = -r\bar{a}_0^2 + i\bar{a}_0^2 2\sigma_r, \quad \text{(C13)}$$

$$A_5 = 2kl|B|b_c(-\bar{a}_0^2 + k^2)\mathrm{e}^{-i\chi} - 2b_c kl, \quad \text{(C14)}$$

$$A_6 = -2kl|B|b_c(-\bar{a}_0^2 + k^2)\mathrm{e}^{i\chi} + 2b_c kl, \quad \text{(C15)}$$

$$A_7 = -r\bar{a}_1^2 + i[\bar{a}_1^2 2\sigma_r + k_1(U\bar{a}_1^2 + \beta)], \quad \text{(C16)}$$

$$A_8 = l(a_{-1}^2 - a_0^2)(k_{-1} - k_0)\mathrm{e}^{i\gamma_{-1}}|L_{-1}|, \quad \text{(C17)}$$

$$A_9 = l(a_1^2 - a_0^2)(k_1 - k_0)\mathrm{e}^{i\gamma_1}|L_1|, \quad \text{(C18)}$$

$$\bar{a}_n^2 = (nk + 2k_0)^2 + 4l^2. \quad \text{(C19)}$$

10. Appendix D

Explicit representation of η and N

The complex constants η and N are,

$$\eta = [S_7(g_5 S_1 - g_2 S_3) - S_5 S_1 g_8]/[S_7(g_4 S_1 - g_1 S_3) - S_5 S_1 g_7], \quad \text{(D1)}$$

$$N = [S_7(g_6 S_1 - g_3 S_3) - S_5 S_1 g_9]/[S_7(g_4 S_1 - g_1 S_3) - S_5 S_1 g_7], \quad \text{(D2)}$$

where,

$$g_1 = a_{-1}^2|L_{-1}|\mathrm{e}^{i\gamma_{-1}}, \quad \text{(D3)}$$

$$g_2 = -\frac{\Delta}{|\Delta|}kl|B|b_c(-a_0^2 + k^2)|L_0|\mathrm{e}^{i(\gamma_0 - \chi)} + \frac{\Delta}{|\Delta|}klb_c\mathrm{e}^{i\gamma_0}|L_0|, \quad \text{(D4)}$$

$$g_3 = -kl|L_0|(k^2 - a_0^2)[|F_B|\mathrm{e}^{i(\gamma_0 - \chi - \zeta)} + Q|M_B|\mathrm{e}^{i(\gamma_0 - \chi - \zeta_B)}] - l|L_0|(\bar{a}_{-1}^2 - a_0^2)(k_{-1} - k_0) f_{-1}^{(2)} - l|L_1|(\bar{a}_0^2 - a_1^2)(k_0 - k_1)\mathrm{e}^{-i\gamma_1} f_0^{(2)}, \quad \text{(D5)}$$

$$g_4 = a_0^2|L_0|, \quad \text{(D6)}$$

$$g_5 = -\frac{\Delta}{|\Delta|}kl|B|b_c(-a_1^2 + k^2)|L_1|\mathrm{e}^{i(\gamma_1 - \chi)} + \frac{\Delta}{|\Delta|}kl|B|b_c(-a_{-1}^2 + k^2)|L_{-1}|\mathrm{e}^{i(\gamma_{-1} + \chi)} + \frac{\Delta}{|\Delta|}klb_c|L_1|\mathrm{e}^{i\gamma_1} - \frac{\Delta}{|\Delta|}klb_c|L_{-1}|\mathrm{e}^{i\gamma_{-1}}, \quad \text{(D7)}$$

$$g_6 = kl|L_{-1}|(k^2 - a_{-1}^2)[|F_B|\mathrm{e}^{i(\gamma_{-1} + \chi + \zeta)} + Q|M_B|\mathrm{e}^{i(\gamma_{-1} + \chi + \zeta_B)}] \quad \text{(D8)}$$

$$- kl|L_1|(k^2 - a_1^2)[|F_B|\mathrm{e}^{i(\gamma_1 - \chi - \zeta)} + Q|M_B|\mathrm{e}^{i(\gamma_1 - \chi - \zeta_B)}], \quad \text{(D9)}$$

$$g_7 = a_1^2|L_1|\mathrm{e}^{i\gamma_1}, \quad \text{(D10)}$$

$$g_8 = \frac{\Delta}{|\Delta|}kl|B|b_c(-a_0^2 + k^2)|L_0|\mathrm{e}^{i(\gamma_0 + \chi)} - \frac{\Delta}{|\Delta|}klb_c|L_0|\mathrm{e}^{i\gamma_0}, \quad \text{(D11)}$$

$$g_9 = kl|L_0|(k^2 - a_0^2)[|F_B|\mathrm{e}^{i(\gamma_0 + \chi + \zeta)} + Q|M_B|\mathrm{e}^{i(\gamma_0 + \chi + \zeta_B)}] - l|L_{-1}|(\bar{a}_0^2 - a_{-1}^2)(k_0 - k_{-1}) f_0^{(2)}\mathrm{e}^{-i\gamma_{-1}} - l|L_0|(\bar{a}_1^2 - a_0^2)(k_1 - k_0) f_1^{(2)}, \quad \text{(D12)}$$

$$S_1 = -ra_{-1}^2 + i[\sigma_r a_{-1}^2 + k_{-1}(-Ua_{-1}^2 + \beta)], \quad \text{(D13)}$$

$$S_2 = -klb_c[1 - |B|(k^2 - a_0^2)\mathrm{e}^{-i\chi}], \quad \text{(D14)}$$

$$S_3 = klb_c[1 - |B|(k^2 - a_{-1}^2)\mathrm{e}^{i\chi}], \quad \text{(D15)}$$

$$S_4 = -ra_0^2 + i[\sigma_r a_0^2 + k_0(-Ua_0^2 + \beta)], \quad \text{(D16)}$$

$$S_5 = -klb_c[1 - |B|(k^2 - a_1^2)\mathrm{e}^{-i\chi}], \quad \text{(D17)}$$

$$S_6 = klb_c[1 - |B|(k^2 - a_0^2)\mathrm{e}^{i\chi}], \quad \text{(D18)}$$

$$S_7 = -ra_1^2 + i[\sigma_r a_1^2 + k_1(-Ua_1^2 + \beta)]. \quad \text{(D19)}$$

REFERENCES

Blackmon, M. L., Madden, R. A., Wallace, J. M. and Gutzler, D. S. 1979. Geographical variations in the vertical structure of geopotential height fluctuations. *J. Atmos. Sci. 36*, 2450–2466.

Burns, A. G. and Maslowe, S. A. 1983. Finite-amplitude stability of a zonal shear flow. *J. Atmos. Sci. 40*, 3–9.

Buzzi, A., Trevisan, A. and Speranza, A. 1984. Instabilities of a baroclinic flow related to topographic forcing. *J. Atmos. Sci. 41*, 637–650.

Charney, J. G. and Eliassen, A. 1949. A numerical method for predicting the perturbations of the middle latitude westerlies. *Tellus 1, No. 2*, 38–54.

Charney, J. G. and DeVore, J. G. 1979. Multiple flow equilibria in the atmosphere and blocking. *J. Atmos. Sci. 36*, 1205–1216.

Charney, J. G. and Flierl, G. R. 1981. Oceanic analogues of large-scale atmospheric motions. In *Evolution of physical oceanography* (eds. B. A. Warren and C. Wunch). MIT Press, 504–548.

Deininger, R. C. 1981. Topographically forced wave instability at finite amplitude. *J. Atmos. Sci. 38*, 2619–2625.

Drazin, P. G. 1972. Nonlinear baroclinic instability of a continuous zonal flow of viscous fluid. *J. Fluid Mech. 55*, 577–587.

Egger, J. 1976. The linear response of a hemispheric two-level primitive equations model to forcing by topography. *Mon. Wea. Rev. 104*, 351–364.

Grose, W. L. and Hoskins, B. J. 1979. On the influence of orography on large-scale atmospheric flow. *J. Atmos. Sci. 36*, 223–234.

Hart, J. E. 1979. Barotropic quasi-geostrophic flow over anisotropic mountains. *J. Atmos. Sci. 36*, 1736–1746.

Held, I. M. 1983. Stationary and quasi-stationary eddies in the extratropical troposphere: Theory. In *Large-scale dynamical processes in the atmosphere* (eds. B. Hoskins and R. Pearce). Academic Press, 127–168.

Holopainen, E. O. 1978. On the dynamic forcing of the long-term mean flow by the large-scale Reynold's stresses in the atmosphere. *J. Atmos. Sci. 35*, 1596–1604.

Itoh, H. 1985. The role of transient motions in the formation of quasi-stationary planetary waves. *J. Atmos. Sci. 42*, 917–932.

Landau, L. D. 1944. On the problem of turbulence. *C. R. Acad. Sci. U.R.S.S. 44*, 311–314.

Lau, N.-C. 1979. The observed structure of tropospheric stationary waves and the local balances of vorticity and heat. *J. Atmos. Sci. 36*, 996–1016.

Li, G.-Q., Kung, R. and Pfeffer, R. L. 1986. An experimental study of baroclinic flows with and without two-wave bottom topography. *J. Atmos. Sci.*, in press.

Lorenz, E. N. 1972. Barotropic instability of Rossby wave motion. *J. Atmos. Sci. 29*, 258–264.

Pedlosky, J. 1970. Finite-amplitude baroclinic waves. *J. Atmos. Sci. 27*, 15–30.

Pedlosky, J. 1979. *Geophysical fluid dynamics*. Springer-Verlag, 624 pp.

Reinhold, B. R. 1986. Structural determinism of linear baroclinic waves and simple nonlinear equilibration. *J. Atmos. Sci. 43*, 1484–1504.

Roads, J. O. 1982. Forced, stationary waves in a linear, stratified quasi-geostrophic atmosphere. *J. Atmos. Sci. 39*, 2431–2449.

Romea, R. D. 1977. The effects of friction and β on finite amplitude baroclinic waves. *J. Atmos. Sci. 34*, 1689–1695.

Simmons, A. J., Wallace, J. M. and Branstator, G. W. 1983. Barotropic wave propagation and instability, and atmospheric teleconnection patterns. *J. Atmos. Sci. 40*, 1363–1392.

Tung, K. K. 1976. On the convergence of spectral series—a reexamination of the theory of wave propagation in distorted background flows. *J. Atmos. Sci. 33*, 1816–1820.

Vallis, G. K. 1985. Instability and flow over topography. *Geophys. Astrophys. Fluid Dyn. 34*, 1–38.

Wallace, J. M. 1983. The climatological mean stationary waves: Observational evidence. In *Large-scale dynamical processes in the atmosphere* (eds. B. Hoskins and R. Pearce). Academic Press, 27–53.

Youngblut, C. and Sasamori, T. 1980. The nonlinear effects of transient and stationary eddies on the winter mean circulation. Part I: Diagnostic analysis. *J. Atmos. Sci. 37*, 1944–1957.